

Thermal Stress Analysis of Numi Baffle

Bob Wands

Introduction and Summary

The Numi horn is protected from stray beam with a cylindrical aluminum baffle, 30 cm in diameter, 117 cm long, with a 1 cm diameter hole through the center. This analysis determines the temperature and stress in the baffle due to the deposition of five beam pulses impinging on the baffle at a radius of 1 cm.

The results show that the maximum temperature rise, reached at the end of the fifth pulse, is 235 deg. The maximum stress is 340 MPa (49.3 ksi). This exceeds the yield of the baffle material, but is within acceptable limits for a secondary thermal stress as specified in the ASME Boiler and Pressure Vessel Code.

Finite Element Model

The finite element is shown in Fig. 1. Twenty-node solid elements are used for both temperature and stress analyses. Due to symmetry, a half-model was used, with approximately 226000 nodes and 53000 elements.

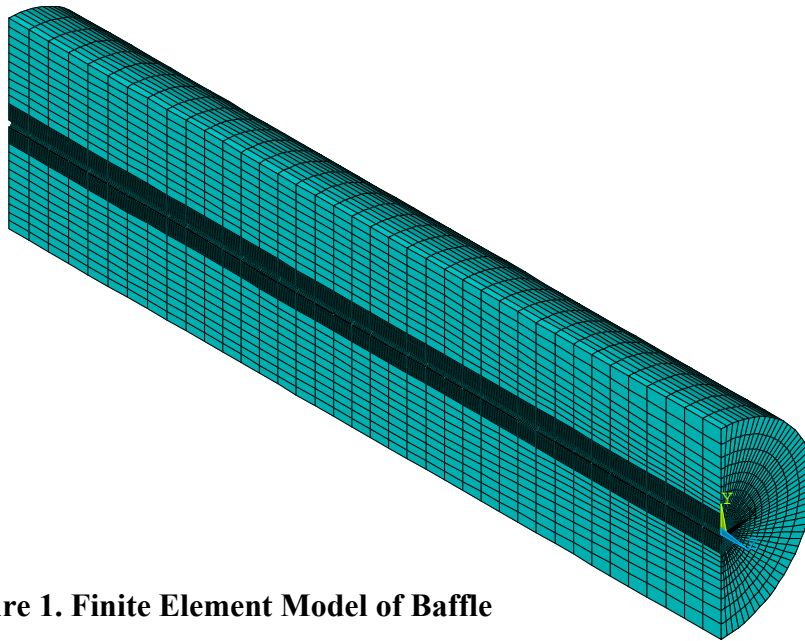


Figure 1. Finite Element Model of Baffle

The following material properties were assumed:

| | |
|--------------------------------------|-----------------------|
| Young's modulus: | 68.9 GPa |
| Coefficient of thermal expansion: | 0.239E-4 m/m-°C |
| Coefficient of thermal conductivity: | 2700 W/m-°C |
| Density: | 235 kg/m ³ |

Loading, in the form of volumetric heat generation, was based on an energy deposition per pulse 221 kJ over a period of 10 μ sec, with a subsequent rest between pulses of 1.9 seconds. A total of 5 pulses were considered, on the assumption that the fault condition will be detected well before this number of pulses actually occurs.

The energy deposition was given in polar coordinates, and input to the finite element program as a table from which each element of the model could "look up" the appropriate energy deposition rate (in W/m³) based on its coordinates in space.

The thermal boundaries were considered adiabatic, i.e., no heat enters or leaves the model across the boundaries.

The temperature profile from the thermal analysis was input to the same finite element model, after the element type was switched from a thermal brick to a structural brick. The structural model was constrained only enough to prevent rigid body motions (Sometimes called "kinematic constraint"). This means that no support reactions can be produced due to thermal expansion.

Results

Thermal Analysis

Fig. 2 shows the maximum baffle temperature as a function of time. The 10 μ sec pulse of heat was input as a square wave, so the rate at which temperature rises is linear over the pulse. Similarly, the interval with no particle beam impingement, being just a special case of square wave, also shows a linear temperature change.

The maximum temperature of 260 °C is reached on the last pulse, at $t = 7.60001$ seconds, and at a distance of about 0.4 m from the upstream face of the baffle Fig. 3 shows the temperature distribution along the length of the baffle. Fig. 4 shows the temperature distribution through the plane of maximum temperature.

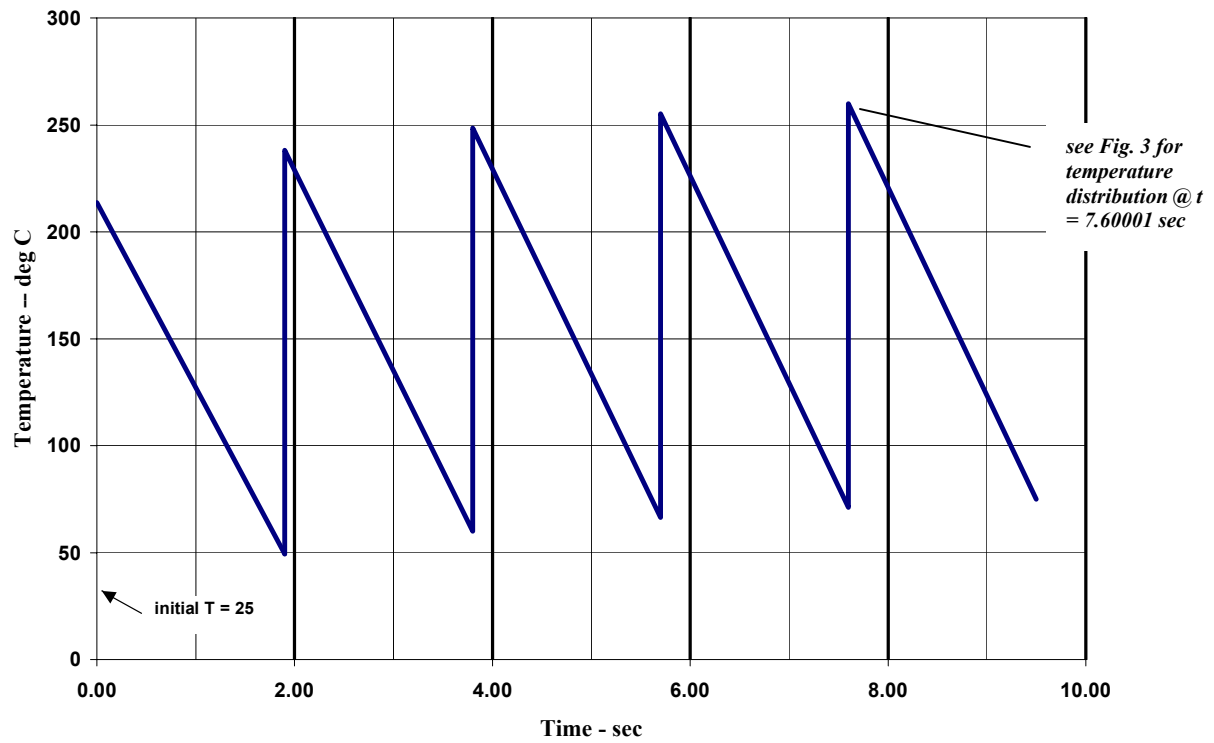


Figure 2. Temperature in Baffle as Function of Time over Five Pulses

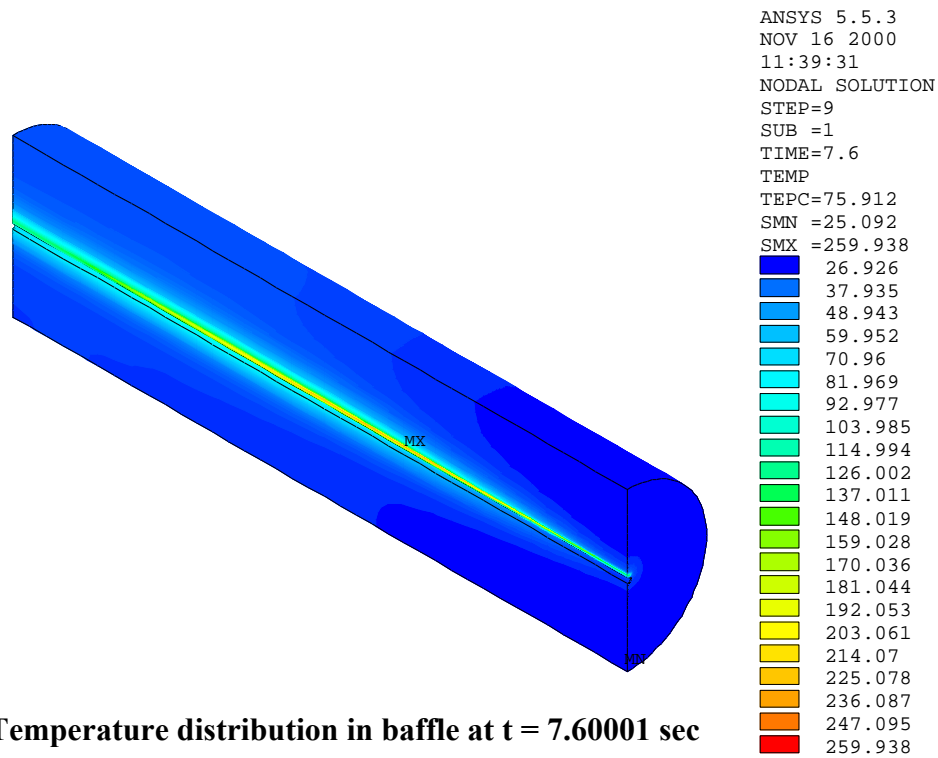


Figure 3. Temperature distribution in baffle at t = 7.60001 sec

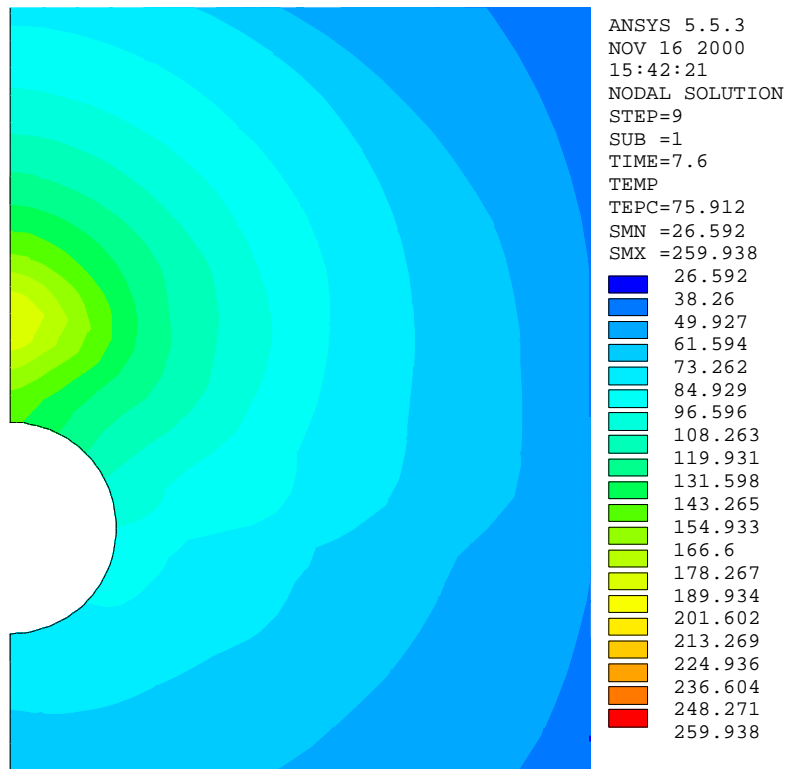


Figure 4. Temperature distribution in plane of maximum temperature – $t = 7.60001$ sec

Stress Analysis

The stress intensity in the baffle is shown in Fig. 5. A slice along a diameter in the plane of the maximum stress is shown in Fig. 6.

The maximum stress intensity is 340 MPa (49.3 ksi), and occurs at a radius of 1 cm, which is the radius at which the beam strikes the collimator. Assuming a minimum specified yield of 240 MPa (35 ksi) for 6061-T6 aluminum, it is clear that yielding occurs.

The volume the finite elements containing stresses in excess of 240 MPa is approximately 25 cm^3 . This volume is located between $z = 0.06 \text{ m}$ and $z = 0.8 \text{ m}$, at $\theta = 90^\circ$ (the location of the beam). The volume of plastic material has a maximum radial thickness of about 6 mm.

Fig. 7 shows the variation of stress intensity with axial location at a radius of 1 cm. The maximum stress occurs at $z = 0.3 \text{ m}$. The temperature along this same path is also plotted, and correlates well with the stress distribution.

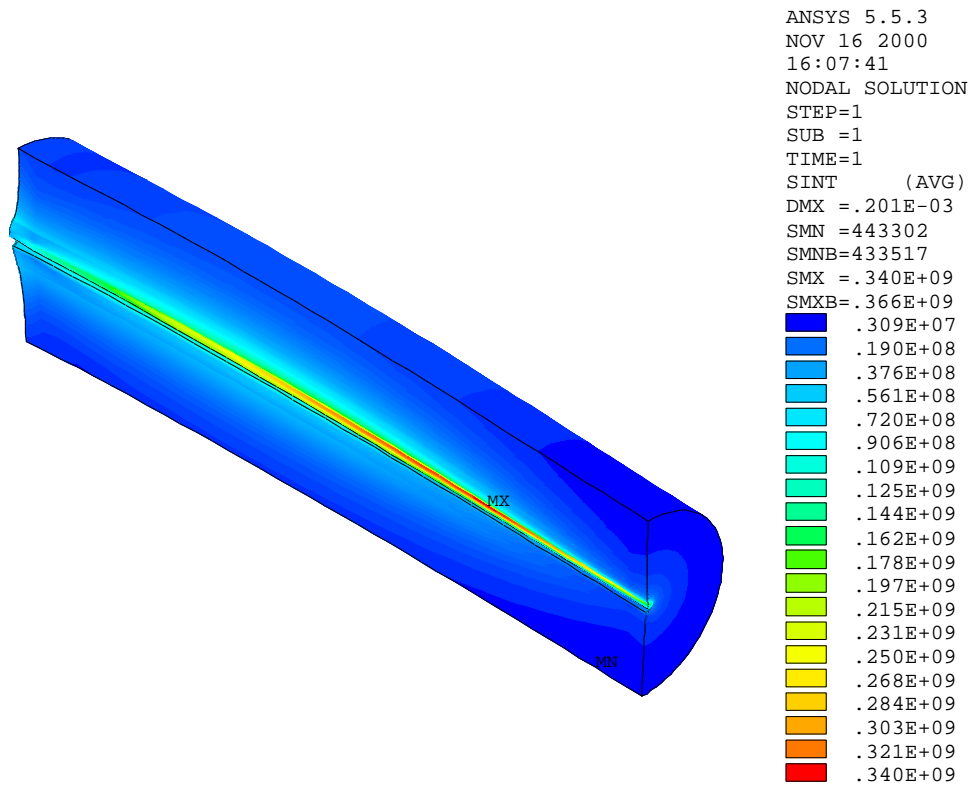


Figure 5. Stress Intensity at Maximum Temperature

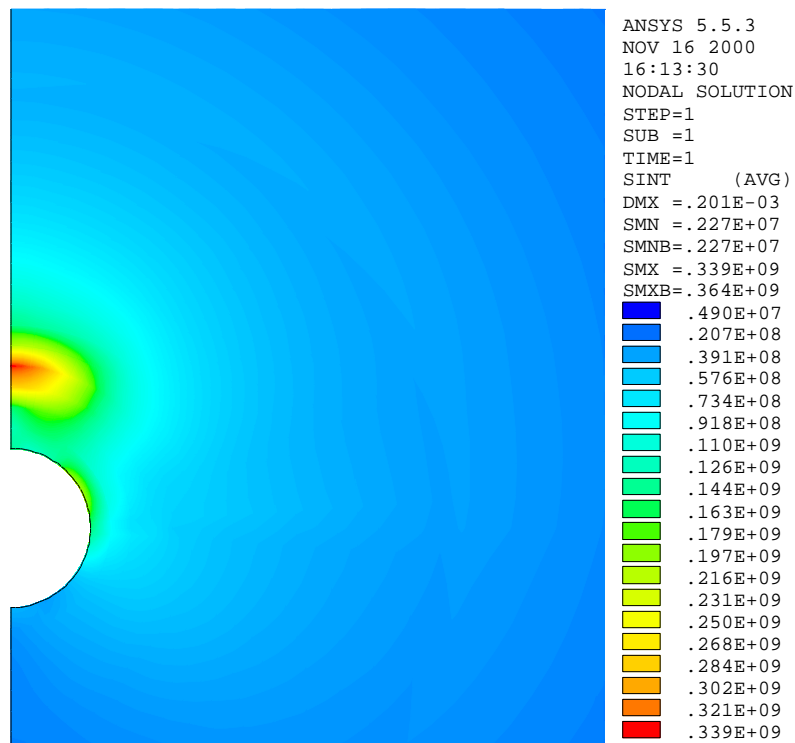


Figure 6. Stress Intensity in Plane of Maximum Stress - Pa

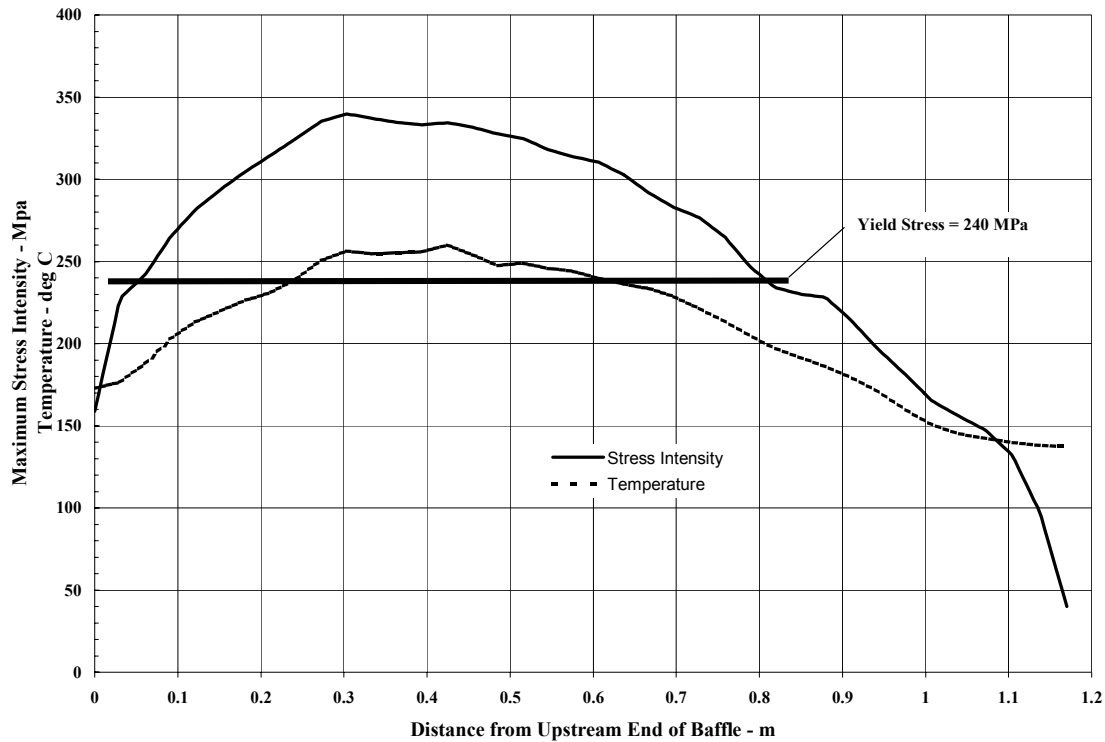


Figure 7. Stress Intensity and Temperature at a radius of 1 cm

The largest deformation is about 0.2 mm, and is in the axial direction. A close look at the results shows that the hot region contains compressive axial, radial, and azimuthal stresses, which is expected from the resistance to expansion provided by the surrounding material. This is in fact a favorable state, in that a close approximation to a hydrostatic stress state is achieved, and the amount of yielding minimized.

Establishing a stress limit for a thermal stress of this nature is problematic. The ASME Boiler and Pressure Vessel Code, Section VIII, Div. 2, allows secondary thermal stresses such as this to reach up to twice the yield stress. This limit assures that thermal ratcheting (progressive elongation with consecutive cycles) does not occur.

The reason for this is shown in Fig. 8. A secondary stress is by definition a stress occurring in a small volume of material within a much larger volume of material which remains elastic throughout the load cycle. When a load is applied, the secondary stress region yields (point B), and continues to strain plastically until the load is a maximum (point C). Upon unloading, the large elastic mass essentially controls the strain of the secondary stress region, and the strain returns to zero. Any plasticity is then reversed, and

strain hardening results, such that subsequent cycles will occur along the line CD, without further plasticity.

(It should be noted that a linear FEA of a plastic region such as this does not give accurate stresses. However, because of the strain-control provided by the large surrounding elastic material, the *strains* are accurate, and stress limits are best understood as strain limits, as Fig. 8 implies.)

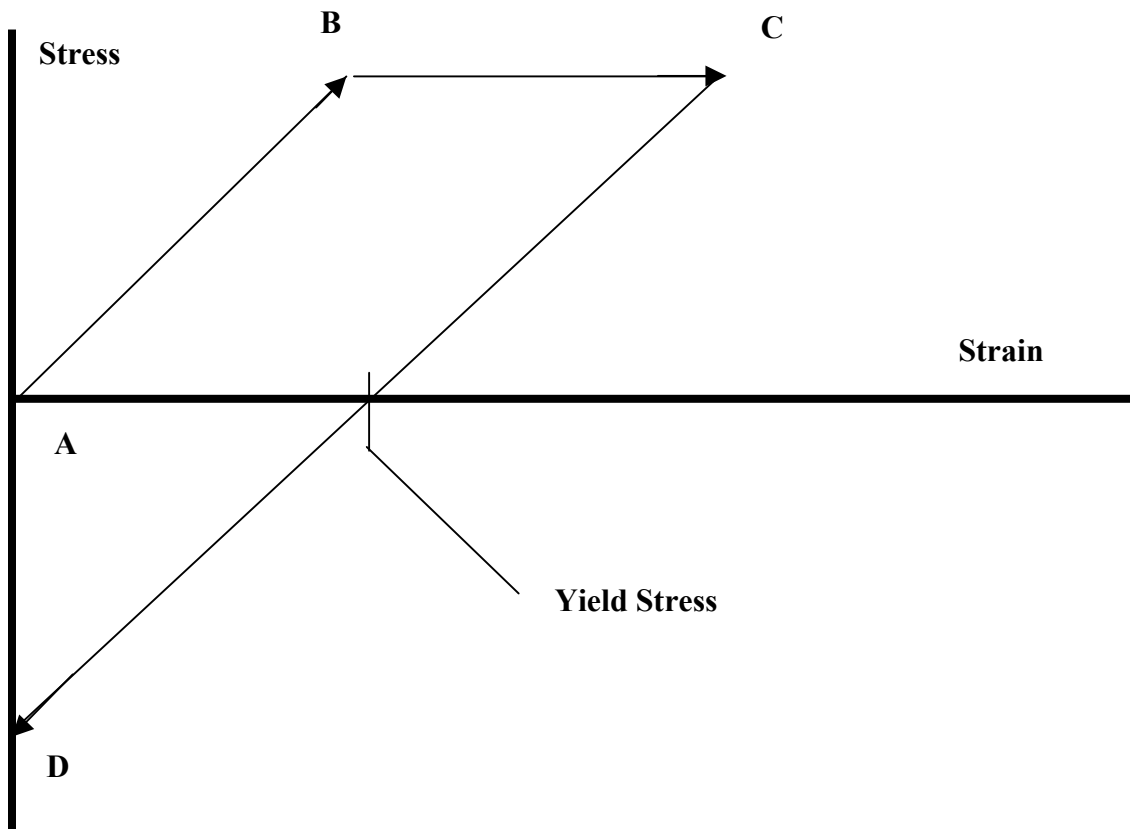


Figure 8. Schematic Representation of Material Behavior in Regions of Strain-Controlled Secondary Stress

Conclusion

The collimator will see a temperature rise of 235 deg. C at the end of five pulses. Stresses will exceed 210 MPa (35 ksi) in a small volume of material at the radius of the beam incidence. Given the small amount of material involved, the stress will have the characteristics of a secondary thermal stress. Secondary thermal stress limits are allowed by ASME Section VIII, Div. 2 to reach up to twice the yield stress, or 480 MPa, well above the maximum stress calculated in this analysis.